

# Additive Effects of Mitochondrion-targeted Cytochrome CYP2E1 and Alcohol Toxicity on Cytochrome *c* Oxidase Function and Stability of Respirosome Complexes\*

Received for publication, October 17, 2011, and in revised form, February 29, 2012. Published, JBC Papers in Press, March 6, 2012, DOI 10.1074/jbc.M111.314062

Seema Bansal<sup>†1</sup>, Satish Srinivasan<sup>†1</sup>, Sureshkumar Anandasadagopan<sup>‡</sup>, Anindya Roy Chowdhury<sup>‡</sup>, Venkatesh Selvaraj<sup>‡</sup>, Balaraman Kalyanaraman<sup>§</sup>, Joy Joseph<sup>§</sup>, and Narayan G. Avadhani<sup>‡2</sup>

From the <sup>†</sup>Department of Animal Biology and the Mari Lowe Center for Comparative Oncology, School of Veterinary Medicine, University of Pennsylvania, Philadelphia, Pennsylvania 19104 and the <sup>§</sup>Department of Biophysics and Free Radical Research Center, Medical College of Wisconsin, Milwaukee, Wisconsin 53226

**Background:** Alcohol toxicity affects mitochondrial function, which likely is a contributing factor in tissue injury.

**Results:** Cytochrome *c* oxidase is the primary target of CYP2E1-mediated alcohol toxicity and oxidative stress.

**Conclusion:** Damage to cytochrome oxidase affects respirosome complexes, which in turn may be the cause of increased ROS production.

**Significance:** Identification of targets of alcohol toxicity and reversing the damage by mitochondrion-targeted antioxidants.

Alcohol treatment induces oxidative stress by a combination of increased production of partially reduced oxygen species and decreased cellular antioxidant pool, including GSH. Recently, we showed that mitochondrion-targeted CYP2E1 augments alcohol-mediated toxicity, causing an increase in reactive oxygen species production and oxidative stress. Here, we show that cytochrome *c* oxidase (CcO), the terminal oxidase of the mitochondrial respiratory chain, is a critical target of CYP2E1-mediated alcohol toxicity. COS-7 and Hep G2 cell lines expressing predominantly mitochondrion-targeted (Mt<sup>++</sup>) CYP2E1 and livers from alcohol-treated rats showed loss of CcO activity and increased protein carbonylation, which was accompanied by a decline in the steady state levels of subunits I, IV1, and Vb of the CcO complex. This was also accompanied by reduced mitochondrial DNA content and reduced mitochondrial mRNA. These changes were more prominent in Mt<sup>++</sup> cells in comparison with wild type (WT) CYP2E1-expressing or ER<sup>+</sup> (mostly microsome-targeted) cells. In addition, mitochondrion-specific antioxidants, ubiquinol conjugated to triphenyl phosphonium, triphenylphosphonium conjugated carboxyl proxyl, and the CYP2E1 inhibitor diallyl sulfide prevented the loss of CcO activity and the CcO subunits, most likely through reduced oxidative damage to the enzyme complex. Our results suggest that damage to CcO and dissociation of respirosome complexes are critical factors in alcohol-induced toxicity, which is augmented by mitochondrion-targeted CYP2E1. We propose that CcO is one of the direct and immediate targets of alcohol-induced toxicity causing respiratory dysfunction.

Excessive and chronic alcohol consumption leading to liver damage and alcohol liver disease is known to elicit a multitude of effects on the hepatic tissue as well as other tissues of the body. It is becoming increasingly apparent that the hepatic mitochondrial compartment is an important target of alcohol toxicity. Studies have linked alcohol-mediated effects to mitochondrial dysfunction, apoptosis, increase in ROS<sup>3</sup> production, loss of cellular ATP, and eventually mitochondrial DNA (mtDNA) damage (1–8). mtDNA encodes 13 proteins associated with the mitochondrial OXPHOS complexes, and it is highly susceptible to oxidative damage (3, 4, 9). Inefficient mtDNA repair and the proximity of mtDNA to the mitochondrial respiratory chain, which is the main site of ROS formation, are thought to be important factors (10–14) in alcohol-induced toxicity.

A number of studies using both cellular and animal models have shown that mitochondrial electron transport chain activities are altered by alcohol treatment. Some studies suggest that complex I and complex II are altered in hepatocytes in various liver pathologies (15, 16), whereas the others consider complex II to be the most resistant complex, which is not damaged even in liver cirrhosis (3, 4, 17–19). Cytochrome *c* oxidase (CcO) is the terminal oxidase of the electron transport chain and contains three large catalytic subunits (I, II, and III) encoded in the mitochondrial genome and up to 10 smaller subunits encoded in the nuclear genome. Several studies over the past decade have reported different types of effects of alcohol on CcO activity in cell culture and animal models. In one of the earliest studies, Lieber and co-workers (20) showed that alcohol treat-

\* This work was supported, in whole or in part, by National Institutes of Health Grants AA-017749 and ARRA supplement to GM-34883. This work was also supported by an endowment from the Harriet Ellison Woodward Foundation.

<sup>1</sup> Both authors contributed equally to this work.

<sup>2</sup> To whom correspondence should be addressed. Tel.: 215-898-8819; Fax: 215-573-6810; E-mail: Narayan@vet.upenn.edu.

<sup>3</sup> The abbreviations used are: ROS, partially reduced O<sub>2</sub> species; CcO, cytochrome *c* oxidase; Mito-Q, ubiquinol conjugated to triphenyl phosphonium; Mito-CP, triphenylphosphonium conjugated carboxyl proxyl; DAS, diallylsulfide; BNG, Blue Native gel; DNP, 2,4-dinitrophenol; BisTris, 2-[bis(2-hydroxyethyl)amino]-2-(hydroxymethyl)propane-1,3-diol; OCR, oxygen consumption rate; Tricine, *N*-[2-hydroxy-1,1-bis(hydroxymethyl)ethyl]glycine; ER, endoplasmic reticulum; NAC, *N*-acetylcysteine; CYP2E1, cytochrome P4502E1.

ment in baboons resulted in markedly altered hepatic mitochondrial CcO activity. Similarly, exposure of mitochondrial membrane fractions with alcohol caused the structural perturbation of the a3-CuB site, affecting CcO activity (21). Another study showed that hepatic mitochondrial NO levels markedly increased under chronic alcohol treatment (22, 23), which covalently modified the heme moiety leading to reduced CcO activity. CcO gene expression and CcO activity were also impaired in chick embryonic cardiac myocytes (24) following alcohol treatment. However, the details of mechanisms of alcohol effects on the CcO complex and the precise subunits affected remain unclear.

It is known that some selective subunits of the CcO complex are degraded under oxidative stress conditions, experimental or chemical hypoxia, myocardial ischemia, or pathological conditions such as cancer (25–31). A previous study from our laboratory showed a steady and notable loss of subunits I, IV1I, and Vb under chemical stress, hypoxia, and myocardial ischemia/reperfusion conditions (28, 31, 32). Others have shown lowering of subunits I, II, and VIc in addition to subunits IV1I and Vb (33) under different pathophysiological conditions.

The cytochrome CYP2E1 catalyzes the metabolism of numerous xenobiotics, industrial chemicals, and alcohol (34–35). Several studies implicate CYP2E1 in alcohol toxicity and alcohol liver disease, although the precise mechanism and subcellular target(s) remain unclear. Notably, CYP2E1 is induced in the liver and several extrahepatic tissues by small organic molecules such as ethanol, pyrazole, acetone, or isoniazide (36–39). Consequently, the tissue levels of this heme protein are significantly increased following alcohol consumption. The increased tissue level of CYP2E1 appears to have an additive effect on alcohol toxicity (34–37, 40). In a recent study, we showed that mitochondrion-targeted CYP2E1 markedly augmented ethanol-induced toxicity and oxidative stress in COS cells (40), whereas the microsomal-targeted CYP2E1 had a marginal effect in mediating alcohol toxicity. In this study, we show that the catalytic function of CYP2E1 during alcohol treatment is a key factor in modulating the activities of mitochondrial electron transport chain complexes, in particular, the CcO complex and retention of electron transfer chain super complexes called respirosomes. Inhibitors of CYP2E1 or mitochondrion-targeted antioxidants alleviated the alcohol-induced effect providing a direct link between the metabolic activity of mitochondrial CYP2E1 and loss of CcO activity. Our results show a cumulative effect of mitochondrial CYP2E1 and alcohol on mitochondrial dysfunction that appears to represent a major part of alcohol toxicity.

## EXPERIMENTAL PROCEDURES

**Cell Culture and Alcohol Treatment**—COS-7 cells (ATCC, CRL, and 1651) and Hep G2 cells (ATCC CRL-10741) were cultured in Dulbecco's modified Eagle's medium (DMEM) supplemented with 10% fetal bovine serum (v/v) in the presence of added 1% penicillin/streptomycin. Preparation of COS cells stably expressing CYP2E1 constructs was described before (40). Transduction of Hep G2 cells with WT and Mt<sup>++</sup> CYP2E1 cDNAs cloned in pBABE retroviral vector and selection of positive clones were as described for COS cells (40). COS cells were

treated with ethyl alcohol, hereafter referred to as alcohol, at a concentration of 25–100 mM, and Hep G2 cells were treated with 300 mM alcohol. Cultures were fed each day for a maximum of 2 days (48 h) in the case of COS cells and 4 days (96 h) in the case of Hep G2 cells with alcohol containing fresh media to establish the peak alcohol concentration needed for inducing the toxic effects (40). We did not see significant cell death under these conditions.

**Animal Feeding Experiments**—Sprague-Dawley rats (about 150 g) were fed with alcohol for 2, 4, 6, 8, and 10 weeks, and pair-fed controls received isocaloric diet. The standard procedure for alcohol feeding was based on the Lieber De Carli protocol (40, 41). Animals were fed *ad libitum* a nutritionally balanced liquid diet containing 2–36% caloric equivalent of ethanol, 18% protein, 35% fat, and 11% carbohydrate as % of total calories (supplied by BioServe Corp., San Diego). The ethanol content was steadily increased from a caloric equivalent of 2–4% during the 1st week to 36% by the 4th week and then maintained at this level until 10 weeks. Control pair-fed animals received the same diet except that alcohol was isocalorically replaced by maltose dextrins. Feeding was carried out in the Animal Resource Facility of Thomas Jefferson University Medical College, Philadelphia, under their approved animal care protocol.

**Preparation of Mitochondrial Extracts**—Mitochondria from cultured cells and freshly extracted rat livers were prepared by differential centrifugation as described previously (32, 40). Cells were washed with cold PBS and homogenized with a Dounce glass homogenizer in H-medium (70 mM sucrose, 220 mM mannitol, 2.5 mM Hepes, pH 7.4, 2 mM EDTA, and Complete Protease Inhibitor Mixture). Livers were perfused with phosphate-buffered saline, and rinsed with the same buffer before use. Livers were sliced and homogenized in a Glass Col motor-driven glass-Teflon homogenizer as described before (32, 40). Mitochondria and microsomes were prepared by differential centrifugation and suspended in 20 mM K<sub>2</sub>HPO<sub>4</sub> buffer containing 20% glycerol with added leupeptin, pepstatin, antipain, and PMSF. Protein concentration of cell fractions were determined by the method of Lowry *et al.* (42), and aliquots were stored at –80 °C until use.

**Analysis of Cellular O<sub>2</sub> Consumption in a Seahorse XF24 Respirometer**—Oxygen consumption rates (OCR) were measured using the XF24 high sensitivity respirometer (Seahorse Bioscience) as described by Wu *et al.* (43) following the manufacturer's instructions. Briefly, 20,000 cells were cultured in DMEM for 16 h and changed with XF assay medium, low buffered bicarbonate-free DMEM, pH 7.4, for 1 h before the measurement. The final concentrations of inhibitors used were 2 μg/ml oligomycin, 40 μM of the uncoupler 2,4-dinitrophenol (DNP) for ER<sup>+</sup> cells and 50 μM for WT and Mt<sup>++</sup> cells, and 1 μM of the complex I inhibitor, rotenone. The plate along with the cartridge was loaded into the XF analyzer. OCR was measured under basal conditions and after sequential addition of oligomycin, DNP, and rotenone. All respiration rates were calculated as percentage of the rate. The difference in the cell density between wells is corrected by loading the cell lysate on 12% SDS-PAGE and probing with actin antibody by immunoblot analysis. The absolute rates of oxygen consumption were

## Alcohol-induced Cytochrome Oxidase Dysfunction

linearly related to cell numbers seeded within the measurement range. Respiration rates at each time point from three replicate wells were averaged.

**Assay of Electron Transport Chain Activity**—Assays of complex I–III were essentially as described by Birch-Machin and Turnbull (44) using a Cary 1E UV-visible spectrophotometer. Briefly, complex I activity (NADH:ubiquinone oxidoreductase) was measured by incubating 15  $\mu\text{g}$  of freeze-thawed mitochondrial extract from control and alcohol-treated cells and tissues in 1 ml of assay medium (25 mM potassium phosphate, pH 7.4, 5 mM  $\text{MgCl}_2$ , 2 mM NaCN, 2.5 mg/ml bovine serum albumin, 13 mM NADH, 65  $\mu\text{M}$  ubiquinone, and 2  $\mu\text{g}/\text{ml}$  antimycin A) and measuring the decrease in absorbance at 340 nm because of NADH oxidation. Rotenone sensitive complex I activity was assayed by the addition of 40  $\mu\text{mol}/\text{liter}$  rotenone. Complex II–III activity (succinate-cytochrome *c* reductase) was measured by incubating 20  $\mu\text{g}$  of freeze-thawed mitochondrial extract in 1 ml of assay medium (25 mM potassium phosphate, pH 7.4, 2 mM NaCN, 20 mM succinate, 2  $\mu\text{g}/\text{ml}$  rotenone, and 37.5  $\mu\text{M}$  oxidized cytochrome *c*) and measuring the increase in absorbance at 550 nm because of cytochrome *c* reduction.

CcO activity was measured by incubating 2–10  $\mu\text{g}$  of freeze-thawed mitochondrial extract prepared from control and alcohol-treated (100 mM for 48 h) cells, and tissues in 1 ml of assay medium (25 mM potassium phosphate, pH 7.4, and 0.45 mM dodecyl maltoside). Ferrocycytochrome *c* (15  $\mu\text{M}$ ) was added, and the reaction rates were measured using Cary-1E spectrophotometer. First order rate constants were calculated based on regression analysis using the Cary-Win kinetics software. The  $\epsilon$  of 21.1 was used for the conversion of OD to molar amounts of reduced cytochrome *c* oxidized. In some assays, cells were also treated with Mito-Q (1  $\mu\text{M}$ ), Mito-CP (2  $\mu\text{M}$ ), DAS (10  $\mu\text{M}$ ), or NAC (10 mM) as indicated.

**Measurement of Heme aa3 Content**—Freeze-thawed mitochondrial extract (900  $\mu\text{g}$ ) from control and alcohol-treated rats were incubated on ice for 30 min in 2 ml of 25 mM phosphate buffer, pH 7.4, containing 2% dodecyl maltoside before being split into two cuvettes (28). Sodium ascorbate (10–20 mg) was added to one of the cuvettes, and after 10 min of incubation, the reduced minus oxidized difference spectra from 400 to 800 nm were recorded at room temperature (25  $^\circ\text{C}$ ).

**SDS-PAGE and Blue Native Gel (BNG) Electrophoresis**—For SDS-PAGE analysis, 50  $\mu\text{g}$  of mitochondrial extract was separated on an SDS-12% denaturing polyacrylamide gel. Protein was then transferred to nitrocellulose membranes (Bio-Rad) and stored dry between filter paper until use. Blue native PAGE (39) was carried out essentially as described previously (28). Briefly, 150  $\mu\text{g}$  of mitochondrial protein was solubilized in 30  $\mu\text{l}$  of solubilization buffer containing 1.5 M aminocaproic acid, 50 mM BisTris, and 0.2% dodecyl maltoside and incubated on ice for 30 min. The insoluble material was pelleted by centrifugation at 100,000  $\times g$  for 30 min, and the supernatant was mixed with BNG loading buffer (750 mM aminocaproic acid, 50 mM BisTris, 0.5 mM EDTA, and 5% Serva Blue G) and separated on a 5–16% gradient gel. The gels were run at 100 V, initially with cathode buffer containing the blue dye. When the dye front reached the middle of the gel, the buffer was replaced by a clear cathode buffer. Electrophoresis was carried out until the blue

dye reached the end of the gel. Protein was transferred to PVDF membrane (20 mA for 30 min) and used for immunoblotting.

**Two-dimensional Blue Native Gel and SDS-PAGE Analysis**—The respirosome complexes were resolved by electrophoresis of BNG strips on SDS gels in the second dimension as described by Schagger and von Jagow (45). The technique allows the separation of the multisubunit complexes and the assessment of their *in situ* activity within the gel. Mitochondrial extracts were treated with n-dodecyl- $\beta$ -D-maltoside. This mild detergent allows the separation of respiratory chain complexes while keeping intact their subunit assembly and activity. In the first dimension, the electron transport chain complexes were separated by Blue Native PAGE as described above. 6–13% gradient acrylamide gel was used for resolving intact complexes by Blue Native gel electrophoresis. For the second dimension analysis, individual lanes from the first dimension were excised and incubated for 1 h in a denaturing solution containing 1% SDS and 1% 2-mercaptoethanol. The gel strip was placed at 90 $^\circ$  from its original orientation in the stacking gel area of a 10% Tricine-SDS acrylamide gel as described by Nijtmans *et al.* (46), and standard SDS-PAGE was performed. At the completion of the second dimension run, protein was transferred and probed with antibody against CcO I subunit.

**Measurement of Extracellular  $\text{H}_2\text{O}_2$  by Amplex Red**— $\text{H}_2\text{O}_2$  in cells grown in 96-well plates (hereafter referred to as ROS) was measured using the Amplex Red hydrogen peroxide/peroxidase assay kit from Invitrogen. The method involves the horseradish peroxidase (HRP)-catalyzed oxidation of the colorless and nonfluorescent molecule, *N*-acetyl-3,7-dihydroxyphenoxazine (Amplex Red) to resorufin. The fluorescence was recorded at an excitation of 530 nm and emission at 590 nm in a MicroWin chameleon multilabel detection platform. 15,000 cells were plated in 96-well black bottom plate in phenol-free medium overnight. Alcohol treatment (300 mM) was carried out for 96 h as stated above. Mito-CP at a concentration of 2  $\mu\text{M}$  was also added to the cells for a period of 12 h before measurement.

**Immunoblot Analysis and Source of Antibodies**—Antibody-specific ATPase subunit  $\beta$  (subunit of complex V), CcO I, CcO IV1, and CcO Vb (Mitosciences, Eugene, OR), and the 70-kDa subunit of complex II (Molecular Probes, Carlsbad, CA) were diluted 1:5000. Mouse monoclonal antibody to porin was from Abcam, Cambridge, MA. Polyclonal antibody to DNP moiety was from Millipore, Billerica, MA. Monoclonal antibody specific for CcO II was from Santa Cruz Biotechnology, Santa Cruz, CA. CYP2E1 antibody was from Oxford Biomedicals (Rochester Hills, MI). Blots were probed and developed using the SuperSignal West Femto System (Pierce) and imaged on a Bio-Rad VersaDoc Imaging System and Odyssey Licor (Licor Biotechnology, Lincoln, NE). Digital image analysis was performed using Quantity One Version 4.5 software from Bio-Rad.

**Quantification of Mitochondrial DNA and mRNAs**—Cells were washed extensively with 1 $\times$  phosphate-buffered saline (137 mM NaCl, 2.7 mM KCl, 4.3 mM  $\text{Na}_2\text{HPO}_4$ , 1.47 mM  $\text{KH}_2\text{PO}_4$ , pH 7.4), scraped from the culture dish, and collected by centrifugation at 2000 rpm for 10 min. Total cellular DNA was isolated using Qiagen DNA extraction kit. Total RNA was isolated using TRIzol reagent (Invitrogen) and stored at  $-80^\circ\text{C}$ . Total DNA

and RNA were isolated from freshly harvested rat livers essentially by the same procedure. For real time PCR analysis, RNA was digested with turbo DNase I (Ambion, Inc.), and cDNA was synthesized using the High Capacity cDNA Archive kit (Applied Biosystems). Relative mRNA levels of subunits *CcoI*, *Atpase6*, and *CcoIV* were determined by standard SYBR Green real time PCRs on an ABI 7300 real time PCR machine. The levels of the various CcO transcripts were normalized to  $\beta$ -actin/*Gapdh*, the housekeeping gene, and expressed as % change in relation to  $\beta$ -actin mRNA.

**Extent of Protein Carbonylation of Electron Transfer Chain Complexes**—Mitochondrial membrane complexes solubilized in 0.2% lauryl maltoside containing buffer were resolved by Blue Native polyacrylamide gels as described above. Proteins were electrophoretically transferred to PVDF membrane, and the membrane strips were subjected to in-strip derivatization as described by Conrad *et al.* (47). The membranes were incubated in 10 mM 2,4-dinitrophenylhydrazine in 2 N HCl for 10 min at room temperature (48). The strips were washed twice with 2 M Tris-HCl containing 30% glycerol for 15 min and equilibrated with PBS containing 1% Tween 20 and 5% w/v skim milk powder. The membranes were probed with polyclonal antibody to DNP moiety (1:150 dilution) and infrared dye-conjugated goat anti-rabbit IgG as described for immunoblot analysis.

**Cell Viability Assay**—The viability of cells treated with ethanol was determined using the Guava ViaCount assay. This assay distinguishes between viable and dead cells based on the differential permeability of DNA-binding dyes in the ViaCount reagent (Guava Technologies, Hayward, CA). The assay was carried out using the manufacturer's suggested protocol. Cells treated with and without ethanol were trypsinized post-treatment and stained by mixing with ViaCount reagent at a 1:20 dilution, and the viable cell count was determined using Guava Personal Cytometer and CytoSoft 6.2 software.

**Statistical Analysis**—Statistical significance was determined by an unpaired two-tailed Student's *t* test and paired wherever needed. Results for the cultured stable cells and isolated liver samples are presented as means  $\pm$  S.D. of at least three data points from three different experiments. *p* values  $\leq 0.05$  were considered statistically significant, and *p* values  $\leq 0.001$  were considered highly significant.

## RESULTS

**Effects of Alcohol on Respiratory Capacity of CYP2E1-expressing Cells**—In a recent study (40), we showed that mitochondrion-targeted CYP2E1 had a marked effect on alcohol-mediated toxicity. To evaluate the basis for CYP2E1-induced oxidative stress and cellular toxicity, we measured respiratory parameters in cells expressing WT, ER<sup>+</sup>, and Mt<sup>++</sup> CYP2E1 using Seahorse Extracellular flux analyzer. The construction of COS cell lines stably expressing WT, ER<sup>+</sup> (predominantly ER-targeted), and Mt<sup>++</sup> (predominantly mitochondrion-targeted) CYP2E1 was reported previously (40). The OCR in this experiment signifies ATP-coupled respiration, which was severely affected after alcohol treatment in all cells. Although not shown, DNP caused maximum uncoupled respiration, which was also affected by ethanol treatment. In all cases, the respira-

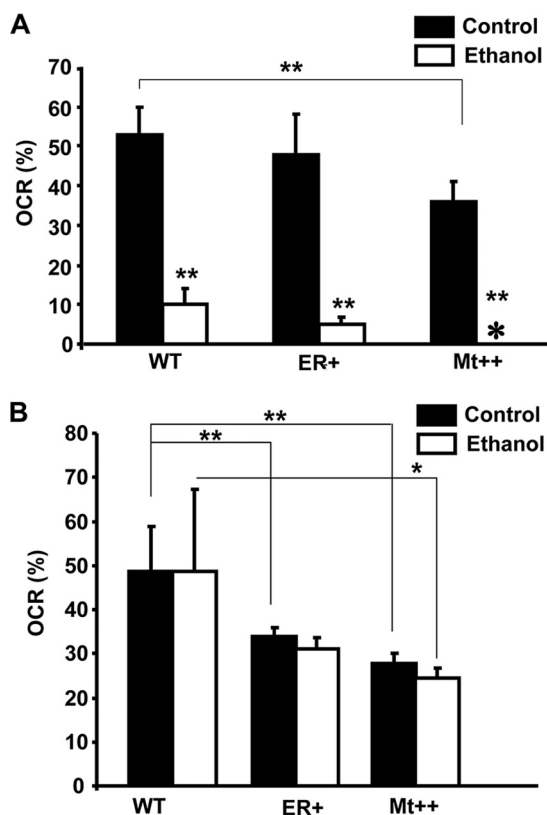


**FIGURE 1. Alcohol-mediated respiratory inhibition in stable cells expressing CYP2E1.** The OCR was measured using the Seahorse Bioscience XF24 extracellular flux analyzer. Control and alcohol-treated cells (20,000 each) were cultured for 16 h followed by a change with XF medium (low buffered bicarbonate-free, pH 7.4) for 1 h before the assay. The plate was incubated without CO<sub>2</sub> for an hour before recording the respiration rates. *A*, %OCR in whole cells grown with or without added 100 mM alcohol for 48 h; *B*, %OCR in cells treated with and without 25 mM alcohol for 48 h. The mean value and S.E. were determined from three separate assays. \* represents *p*  $\leq 0.05$  and \*\* represents *p*  $\leq 0.001$ .

tion was completely inhibited by rotenone, which inhibits complex I and prevents the entry of electrons from NADH into the complex (results not shown). The quantitation of respiration rate (%) presented in Fig. 1A shows that OCR was inhibited markedly in WT, ER<sup>+</sup>, and Mt<sup>++</sup> cells by 100 mM alcohol, although the most severe inhibition was observed in Mt<sup>++</sup> and ER<sup>+</sup> cells. Fig. 1B shows the effects of 25 mM alcohol on the OCR. It is seen that 25 mM ethanol had a marginal effect on OCR in all cells. It is noteworthy that in Fig. 1, *A* and *B*, the basal OCR levels in Mt<sup>++</sup> cells were significantly lower than in WT and ER<sup>+</sup> cells. The results are consistent with our previous results showing induction of respiratory deficiency in yeast cells by mitochondrion-targeted CYP2E1 (40). Results also show that alcohol further augments respiratory deficiency in these cells.

**Effects of Alcohol on the Electron Transport Chain Complexes in CYP2E1-expressing Cells and Livers from Alcohol-treated Rats**—A number of studies have shown the effects of alcohol treatment on the activities of mitochondrial electron transport chain complexes. Here, we investigated the effects of overexpression of mitochondrion- and ER-targeted CYP2E1 on complex I activity (NADH:ubiquinone oxidoreductase), which is a major contributor of ROS, and complex IV activity (cyto-

## Alcohol-induced Cytochrome Oxidase Dysfunction

chrome *c* oxidase), which is the terminal oxidase of the mitochondrial electron transport chain. Results (not presented) show that complex I activity was marginally inhibited in all three cell types expressing different forms of CYP2E1. Alcohol treatment had no significant inhibitory effect on cells expressing WT and ER<sup>+</sup> CYP2E1. However, there was a significant (~20%) inhibition of complex I activity in Mt<sup>++</sup> cells in response to added ethanol. Similar effect was also observed in the alcohol-treated rat livers at 6, 8, and 10 weeks of treatment (results not shown). There was no significant effect at earlier treatment regimens of 2 and 4 weeks. These results suggest a time delayed effect of ethanol treatment on complex I activity. A previous study showed a more pronounced inhibition of complex I activity in ethanol-fed rat livers (9). The difference in activities reported before with the present results likely reflects the methods used for assaying the complex I activity.

Fig. 2A shows the CcO activity in CYP2E1-expressing cells (WT, ER<sup>+</sup>, Mt<sup>+</sup>, and Mt<sup>++</sup>). It is seen that CcO activity was inhibited in all four cell types compared with control cells, although the inhibition was more severe in Mt<sup>+</sup> and Mt<sup>++</sup> cells, which express progressively higher levels of mitochondrion-targeted CYP2E1. Alcohol treatment further exacerbated the inhibitory effect with the highest level of inhibition (60–80%) observed in Mt<sup>++</sup> cells. To study the possible role of CYP2E1 activity and mitochondrial ROS production in alcohol-mediated inhibition of CcO activity, we tested the effects of CYP2E1 inhibitor, DAS, and general as well as mitochondrion-targeted antioxidants, NAC, Mito-CP, and Mito-Q (49, 50), in attenuating the loss of CcO activity. Our results show that NAC prevented alcohol-induced inhibition of CcO activity. Furthermore, Mito-Q and Mito-CP, the two mitochondrion-targeted antioxidants also prevented alcohol-induced loss of CcO activity (Fig. 2B) suggesting that mitochondrially produced ROS may play a direct role in altering the structure/function of CcO enzyme. Interestingly, DAS, an inhibitor of CYP2E1, also rendered protection against alcohol-mediated loss of CcO activity suggesting the importance of the metabolic activity of CYP2E1 in inducing CcO dysfunction. These results are also consistent with the data showing the protective effects of DAS against alcohol-mediated liver injury and depletion of mitochondrial GSH pool when administered to rats and mice (51, 52). We also observed steady decreases in CcO activity in the livers of rats fed an alcohol-containing diet for 2–10 weeks. The decline in CcO activity correlated with increasing hepatic CYP2E1 content, and the most significant and linear decline in CcO activity occurred in rats treated with ethanol for 6, 8, and 10 weeks (Fig. 2C).

**Effects of Alcohol on the Steady State Levels of CcO Subunits**—To understand the molecular basis of decrease in CcO activity in response to alcohol treatment, we carried out immunoblot analysis of mitochondrial membrane fractions from treated and untreated cells and also liver mitochondria from alcohol-treated rats. As shown in Fig. 3A, levels of nuclear-coded CcO IVI1 declined marginally in all CYP2E1-expressing cell types treated with ethanol. The cells transfected with an empty vector (mock-transfected) showed no change in subunit content after alcohol treatment. The decline was rela-

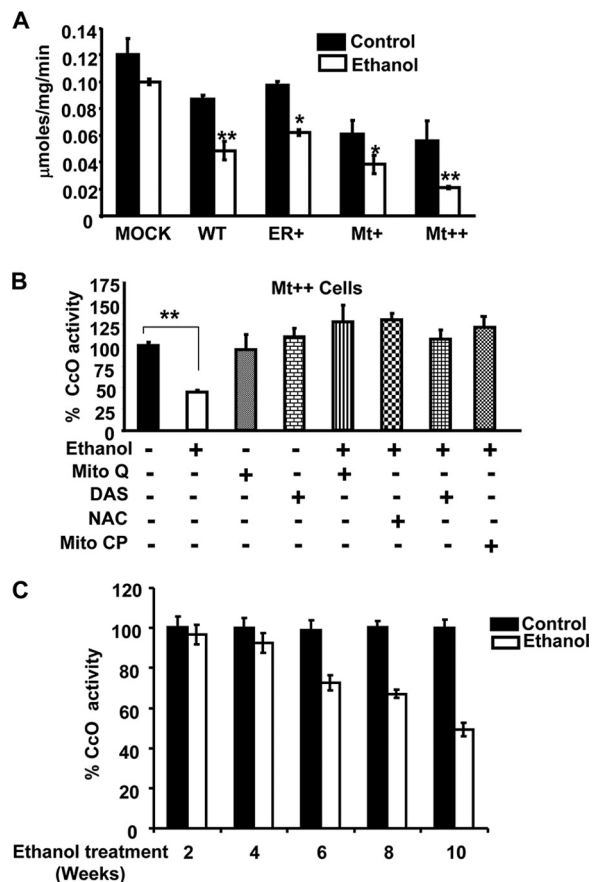


**FIGURE 2. Effects of mitochondrion- and microsomal-targeted CYP2E1 on cytochrome c oxidase activity.** CcO activity was measured by incubating 15 μg of freeze-thawed mitochondrial extract from control and ethanol-treated cells in 1 ml of assay medium (25 mM potassium phosphate, pH 7.4, 0.45 mM dodecyl maltoside, and 15 μM reduced cytochrome *c*). The CcO activity was measured following the rate of decrease in absorbance at 550 nm because of cytochrome *c* oxidation. *A*, relative activities were calculated by taking 2.8 μmol of cytochrome *c* oxidized/min per mg of protein as 100% (*B*). *B*, effects of CYP2E1 inhibitor DAS, NAC, and mitochondrial antioxidants (Mito-CP and Mito-Q) added at zero time along with or without alcohol and incubated for 48 h. The % activity was calculated based on the activity (0.12 mmol/min/mg of protein) of control cells in *A*. *C*, CcO activity of rat liver mitochondria from control and pair-fed rats. Alcohol treatment was carried out for 2–10 weeks as indicated. The activity of liver mitochondria from control rats (6.1 μmol of cytochrome *c* oxidized/min per mg of protein) was considered 100%. Data are presented as ± S.E. from three experiments, and groups were compared using an unpaired, two-tailed Student's *t* test. \* represents  $p < 0.05$  and \*\* represents  $p < 0.001$ .

tively more apparent in ER<sup>+</sup> and Mt<sup>++</sup> cells treated with alcohol compared with WT cells. The steady state levels of subunit Vb (Fig. 3B) declined more markedly in Mt<sup>++</sup> cells, and moderately in ER<sup>+</sup> cells following alcohol treatment. Results also show that pretreatment with DAS or Mito-Q prevented the alcohol-mediated decline of subunit IVI1 and Vb levels in both WT and Mt<sup>++</sup> cells (Fig. 3C). Although not shown, similar effects were observed in Mt<sup>+</sup> cells. These results suggest that the alcohol-mediated decline in CcO activity in CYP2E1-expressing cells is associated with selective loss or degradation of some of the subunits of the complex and that inhibition of CYP2E1 activity or treatment with mitochondrion-targeted antioxidants effectively alleviated this loss. Immunoblot in Fig. 3D shows a similar loss of subunits IVI1 and Vb in liver mitochondria of rats treated with alcohol for 6, 8, and 10 weeks. The

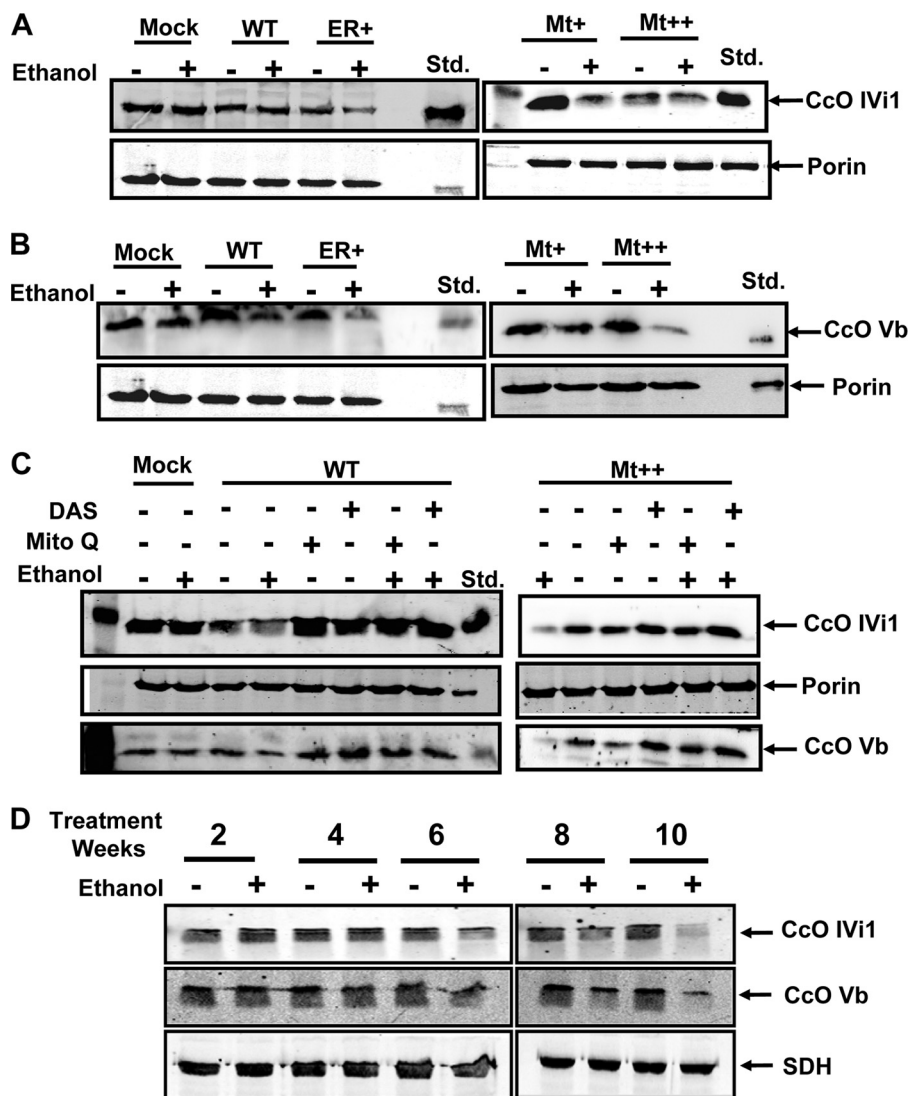


**FIGURE 3. Effects of alcohol treatment on CcO IVI1 and Vb subunit levels.** *A* and *B*, immunoblot analysis of mitochondrial proteins from Mock, ER<sup>+</sup>, WT, Mt<sup>+</sup>, and Mt<sup>++</sup> cell lines treated with and without ethanol (100 mM, 48 h) and rat liver mitochondria from control and alcohol pair-fed rat livers. Proteins (50  $\mu$ g each) were resolved by SDS-PAGE on a 12% gel and subjected to immunoblot analysis with anti-CcO IVI1 and anti-CcOVb antibodies. The blots were also probed with an antibody to the mitochondrion-specific marker succinate dehydrogenase (SDH) or porin as loading controls. *C*, effects of antioxidant Mito-Q (2  $\mu$ M) and CYP2E1 inhibitor DAS (10  $\mu$ M) on the steady state levels of proteins. *D*, rat liver mitochondria from control and pair-fed alcohol (50  $\mu$ g each) were loaded. The blots were imaged through a Li-Cor Odyssey Infrared Imaging System, and the band densities were quantified using the Volume analysis software.

loss of these subunits was minimal in rats from the 2- and 4-week treatment groups. These results suggest that the loss of specific CcO subunits also occurs under *in vivo* conditions. The multiple closely migrating bands IVI1 and Vb likely reflect multiple phosphorylated species.

Consistent with the reduced CcO activity and loss of selective subunits in livers of 6-week alcohol-treated rats, spectral analysis of cholate-solubilized mitochondrial membrane fraction shows a significant reduction in peak at 605 nm characteristic of heme a/a<sub>3</sub>, compared with pair-fed controls. The spectra in Fig. 4 also show that the peak at 548 nm remains unchanged in both alcohol-fed and control liver mitochondria suggesting no change in complex III level. Although not presented, we did not observe a change in complex III activity in CYP2E1-expressing cells as well as alcohol-treated livers.

*Effects of Alcohol Treatment on CcO Complex and Respirosome Complexes*—To further assess the nature of alcohol-induced changes in CcO complexes in WT and Mt<sup>++</sup> cells, we carried out BNG electrophoresis of detergent-solubilized mitochondrial membrane complexes (Fig. 5A) and probed the complexes with antibodies to ATPase  $\beta$  subunit (complex V) and subunit IVI1 of CcO (complex IV). Results of immunoblot (Fig. 5A, upper panel) and quantification of the band density (adjacent panel) show no decline in complex V levels but show a marked decline in complex IV following ethanol treatment. Complex IV levels were lower in Mt<sup>++</sup> cells compared with WT CYP2E1-expressing cells, and a further decline was observed in both cell types following ethanol treatment. Although not shown, there was no significant change in complex I–III levels. These results along with the results of Figs. 2 and 4 suggest that the alcohol toxicity selectively targets com-

## Alcohol-induced Cytochrome Oxidase Dysfunction

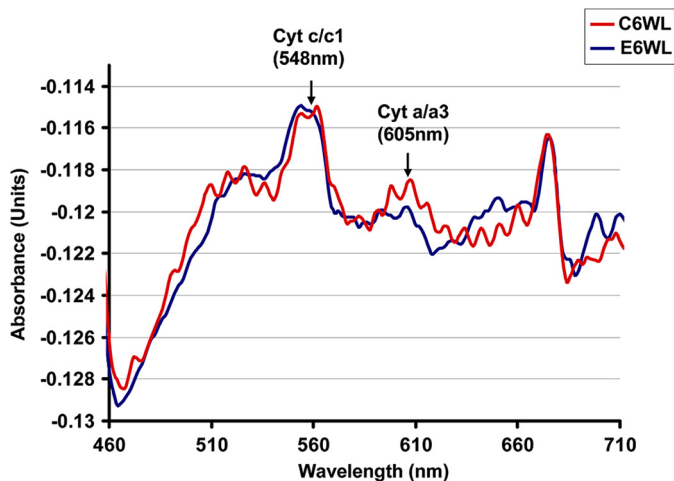


**FIGURE 4. Lower heme a/a3 contents in liver mitochondria from alcohol-treated rats.** Mitochondrial protein (900  $\mu$ g) from rat liver fed with ethanol for 6 weeks was solubilized in 2 ml of 25 mM phosphate buffer, pH 7.4, containing 2% lauryl maltoside, and 1-ml sample of each was distributed in two cuvettes. Dithionite was added in one cuvette. Difference spectrum of reduced minus oxidized sample was recorded in a Cary E1 dual beam spectrophotometer in the range of 400 to 650 nm.

plex IV of the mitochondrial electron transport chain. Consistent with the data on activity patterns and immuno blot patterns of total mitochondrial proteins (Figs. 2 and 3), these results show a reduction in CcO complex in  $Mt^{++}$  cells treated with alcohol.

Two-dimensional BNG electrophoresis pattern in Fig. 5B shows the relative levels of CcO in monomeric complex and S1 to S3 super complexes. Consistent with the results of one-dimensional BNG electrophoresis in Fig. 5A, the aggregate antibody-stained band intensity was lower in cells expressing  $Mt^{++}$  as compared with WT CYP2E1 cells (Fig. 5B). The S1 to S3 super complexes were marginally reduced in WT CYP2E1-expressing cells after ethanol treatment. The levels of these complexes, as well as the monomeric complex, were drastically reduced in  $Mt^{++}$  cells following ethanol treatment, reflecting substantial damage to mitochondrial respirosome assembly. Fig. 5C shows a similar two-dimensional BNG electrophoresis of mitochondrial complexes from 10 weeks of alcohol-fed rat liver and pair-fed control. It is seen that the S1 complex is nearly absent in mitochondria from alcohol-fed rat livers, although S2 was reduced by 50%. The levels of S3 and S4 complexes, however, were decreased by 75%. These results show that respirosome complex assembly is markedly affected in both  $Mt^{++}$  cells and alcohol-fed rat livers.

**Alcohol-mediated Oxidative Damage Preferentially Targets the CcO Complex**—The level of protein carbonylation is a well accepted biomarker for oxidative protein damage. To understand the possible mechanism of alcohol-mediated loss of CcO subunits, we evaluated the extent of protein carbonylation by ROS and other reactive species. In this experiment, mitochondrial electron transfer complexes resolved on BNG were derivatized with 2,4-dinitrophenylhydrazine such that dinitrophenyl hydrazone adducts are formed. The derivatized proteins were then probed with the antibody to the DNP moiety of the protein. In Fig. 6A, we compared complexes from 10 weeks of alcohol-treated rat liver with pair-fed control liver. It is seen that

that the oxidative damage to complexes I and V were nearly similar in control and alcohol-fed livers. The CcO complex, from alcohol-treated livers, however, showed about 1.5-fold higher DNP antibody cross-reactivity suggesting a higher level of damage. Fig. 6B shows the patterns of oxidative damage in WT,  $ER^{+}$ , and  $Mt^{++}$  cells with and without alcohol treatment. It is seen that none of the complexes were stained significantly in WT and  $ER^{+}$  cells even after ethanol treatment suggesting low or minimal oxidative damage to constituent protein subunits. In  $Mt^{++}$  cells, however, the CcO complex was prominently stained with DNP antibody suggesting a high level of oxidative damage. Notably, the CcO complex from ethanol-treated cells was more intensely stained compared with that from untreated cells. It is also seen that other complexes from  $Mt^{++}$  cells were not stained significantly suggesting a more preferential damage to the CcO complex. A companion blot stained with ATPase  $\beta$  subunit antibody as a loading control shows nearly same level of complex V. These results suggest that the loss of CcO subunits in response to alcohol treatment may be related to selective and direct oxidative damage to the complex.

**Effects of Mitochondrion-targeted Antioxidants on mtDNA and Mitochondrial Steady State Transcript Levels**—The levels of mtDNA were measured by PCR amplification of total DNA isolates using *CcoI* and *Atpase6* genes as mitochondrial markers and *CcoIVII* as the nuclear genomic marker. It is seen from Fig. 7A that the levels of mtDNA in 8 weeks of alcohol-fed rat livers is reduced by 30–40%, whereas there was no reduction in the nuclear *CcoIVII* DNA level. Fig. 7, B and C, show the mtDNA contents assayed by PCR amplification of *Atpase6* and *CcoI* genes in cells expressing WT,  $ER^{+}$ , and  $Mt^{++}$  CYP2E1. It is seen that the mtDNA levels in WT and  $Mt^{++}$  cells were nearly similar, although there was a marginal increase in  $ER^{+}$  cells. The reason for this increase in mtDNA remains unclear. The mtDNA contents were significantly lower in all cells following alcohol treatment, although the loss was more severe in  $Mt^{++}$  cells. As expected, the level of nuclear *CcoIVII* DNA did not change in response to alcohol treatment (Fig. 7D). Fig. 7, E and F, show that the steady state levels of *CcoI* and *Atpase6* mRNA were markedly lower in  $Mt^{++}$  cells compared with WT and  $ER^{+}$  cells. This is consistent with higher oxidative stress in these cells. Alcohol treatment further exacerbated this decline more markedly in  $Mt^{++}$  cells, although two other cell types also showed lower transcript levels. Remarkably, DAS, an inhibitor of CYP2E1, and also Mito-CP rendered protection against loss of mtDNA-encoded transcripts. The level of restoration in  $Mt^{++}$  cells was well above the untreated cell level suggesting a higher threshold of oxidative stress in these cells. Although not shown, the levels of *CcoI* and *Atpase6* protein were also restored following treatment with Mito-CP and DAS.

**Alcohol-mediated Toxicity in Hep G2 Cells Expressing Mitochondrial CYP2E1**—The physiological significance of these findings were further assessed in a panel of Hep G2 cells expressing WT and  $Mt^{++}$  CYP2E1 cDNAs. The rationale for the choice of Hep G2 cells was based on tissue origin and also known resistance of these cells to alcohol-induced toxicity. Fig. 8A shows the mitochondrial and microsomal levels of CYP2E1 from mock-transfected, WT, and  $Mt^{++}$  CYP2E1-expressing

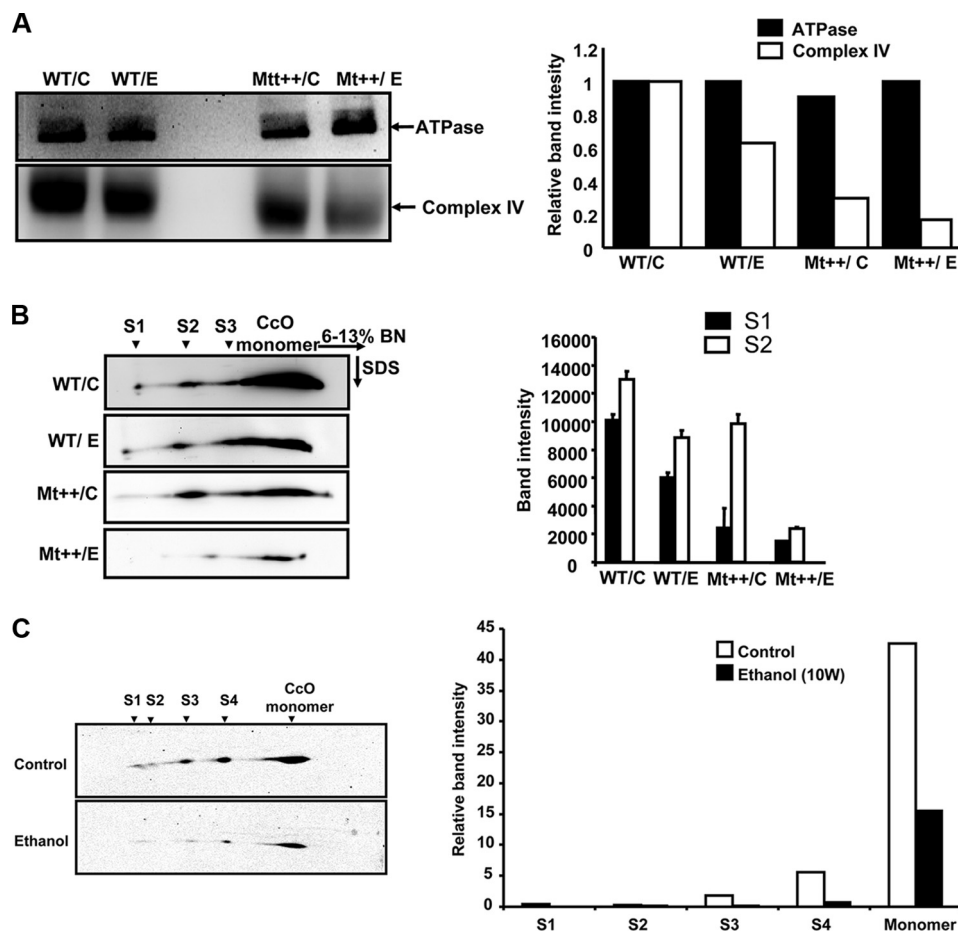


**FIGURE 5. Alcohol-mediated disruption of CcO-containing respirasome complexes in CYP2E1-expressing cells and rat liver mitochondria.** BNG electrophoresis was performed using 150  $\mu$ g of mitochondrial protein solubilized in 0.8% dodecyl maltoside-containing buffer as described under "Experimental Procedures" on a 6–13% acrylamide gradient gel. *A*, proteins from the BNG were transferred to PVDF membrane and probed with antibodies to ATPase  $\beta$  subunit antibody (*upper panel*) and antibody to CcO IV11 subunit (*lower panel*). The *bar diagram* on the *right* shows relative band intensities calculated from the image analysis of blots as described under "Experimental Procedures." The results are average of two representative blots. *B*, two-dimensional Blue Native SDS-PAGE analysis of subcomplexes and also super complexes. Lanes from the BNG electrophoresis were excised and resolved in the second dimension on 10% Tricine gels as described under "Experimental Procedures." The blots were probed with antibody to CcO subunit IV11 to visualize the complexes. The *bar diagram* on the *right* shows relative band intensity of complexes from WT and Mt<sup>+/+</sup> cells treated with or without alcohol. The mean  $\pm$  S.E. values were calculated based on three separate runs. *C*, two-dimensional BNG of rat liver mitochondria from 10 weeks of control rats (*upper panel*) and alcohol fed pairs (*lower panel*). The *bar diagram* at the *bottom* shows relative band intensities of different super complexes quantified as described in *A* and *B* and under "Experimental Procedures." Values in *C* are average of two independent runs.

Hep G2 cells. Similar to what was shown in COS cells, the mitochondrial CYP2E1 content of WT cDNA-transduced cells was about 38%, whereas that of Mt<sup>+/+</sup> cells was about 80%. Also, as shown previously (40), the mitochondrion-targeted CYP2E1 migrated as an ~40-kDa protein possibly because of activation of a cryptic proteolytic site in this mutant protein. As shown previously (40), this N-terminal truncated protein exhibits catalytic activity and heme content similar to full-length CYP2E1 protein.

Fig. 8*B* shows that the CcO activities of WT and Mt<sup>+/+</sup> cells were marginally reduced in comparison with the mock-transfected cells. Alcohol treatment significantly inhibited CcO activity in both mock-transfected and WT CYP2E1-expressing cells. The inhibition was more pronounced in Mt<sup>+/+</sup> cells in response to ethanol treatment. As shown in Fig. 8*C*, the level of CcO subunit IV11 was significantly reduced in both WT and Mt<sup>+/+</sup> CYP2E1-expressing cells following ethanol treatment. As observed in COS cells, the loss of subunit Vb in Mt<sup>+/+</sup> cells treated with ethanol was drastic compared with the mock and WT CYP2E1-expressing cells. It should be noted that the levels

of porin and ATPase  $\beta$  subunits used as loading controls did not significantly vary suggesting that reduced CcO subunit IV11 and Vb is not due to an aberrant derivative process due to cell death. Consistent with this conclusion, the % cell viability of ethanol-treated cells (Fig. 8*D*) did not vary markedly in response to ethanol treatment.

Fig. 8*E* shows the level of H<sub>2</sub>O<sub>2</sub> production measured by Amplex Red method in the three cell lines. Both WT and Mt<sup>+/+</sup> CYP2E1-expressing cells generated a substantially higher level of ROS. Ethanol treatment increased the level, with Mt<sup>+/+</sup> cells producing the highest level. Mito-CP treatment nearly completely abolished ROS production in all three cells. These results further support the role of mitochondrion-targeted CYP2E1 in augmenting alcohol-mediated toxicity and loss of CcO activity.

## DISCUSSION

Despite some early contradictory reports (53), there is compelling evidence that CYP2E1 plays an important role in alco-



## Alcohol-induced Cytochrome Oxidase Dysfunction

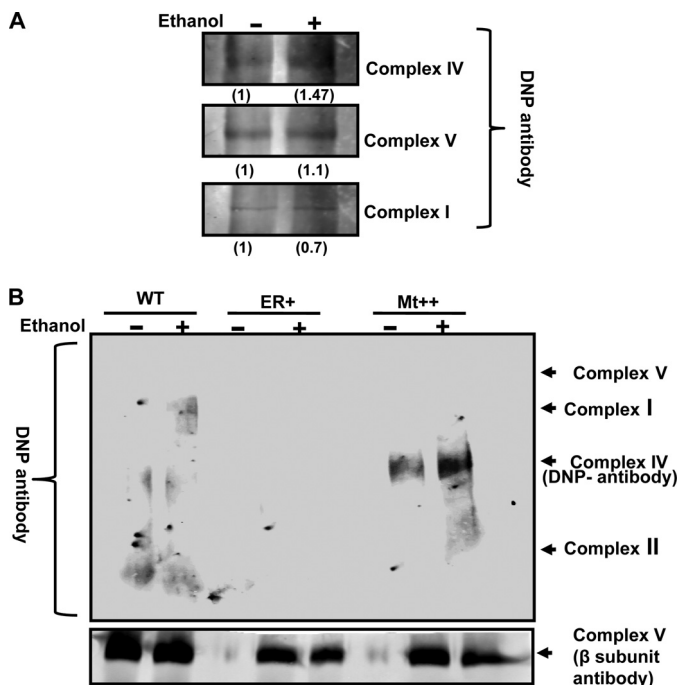


**FIGURE 6. Extent of protein carbonylation of electron transfer complexes from ethanol-fed rats and cells expressing CYP2E1.** Mitochondrial proteins (150  $\mu$ g each) solubilized in sodium maltoside containing buffer were subjected to BNG analysis as described in Fig. 5 and under "Experimental Procedures." Proteins were transblotted to PVDF membrane and subjected to derivatization with 2,4-dinitrophenylhydrazine for the detection of side chain carbonylation by probing with antibody to DNP. **A**, levels of protein carbonylation of different complexes from control and alcohol-fed rat livers. Strips corresponding to indicated complexes were excised and probed with antibody to DNP domain. **B**, complexes from WT, ER<sup>+</sup>, and Mt<sup>++</sup> CYP2E1-expressing cells were resolved by BNG electrophoresis and probed with DNP antibody following derivatization (*upper panel*). The strip corresponding to complex V from an identically run companion blot and probed with ATPase  $\beta$  antibody without derivatization was used as loading control (*lower panel*).

hol-induced toxicity and alcohol liver diseases (54–58). Morgan *et al.* (59) reported that in transgenic mice overexpressing CYP2E1, ethanol administration induced markers of liver injury. Other studies using various transgenic mouse models (60–65) also showed that CYP2E1 expression is a contributing factor in alcohol-mediated liver toxicity. For evaluating the roles of mitochondrion- and ER-targeted CYP2E1, recently we generated cells stably expressing mutant forms of proteins with altered targeting signal properties. CYP2E1 carrying the A2L/A9L mutation was predominantly targeted to the ER, whereas CYP2E1 with the I8R/L11R/L17R mutation was predominantly targeted to mitochondria (40). Using these cell lines, we showed that Mt<sup>++</sup> cells expressing predominantly mitochondrion-targeted CYP2E1 were more vulnerable to alcohol-induced toxicity as observed by their ability to produce markedly higher ROS, increased lipid peroxides (F<sub>2</sub>-isoprostanes), and induced mtDNA depletion in yeast cells. We also showed that the mitochondrion-targeted antioxidant MitoQ and CYP2E1 inhibitor DAS effectively reversed the alcohol-mediated toxicity in these cells. A parallel study by Knockaert *et al.* (66) using a different targeting strategy essentially came to the same conclusion. Using the targeting strategy that was used in our previous study (40) and using two different cell types for expression, we now show that mitochondrial CcO is likely to be the direct and immediate target of alcohol-induced toxicity in Mt<sup>++</sup> cells and

also rat livers treated with alcohol for 6–10 weeks. Our results show selective depletion of CcO IV1 and CcO Vb subunits, which caused disruption of CcO complex and respirasome super complexes. The loss of these subunits is most likely because of increased protein degradation because the CcO IV1 and Vb mRNA levels remain the same in alcohol-treated rat livers and CYP2E1-expressing cells (Fig. 7A and data not shown).

The use of Seahorse micro-respiratory system in this study showed that OCR was markedly reduced in Mt<sup>++</sup>-expressing COS cells as compared with ER<sup>+</sup> and WT cells. Furthermore, alcohol treatment markedly reduced OCR in Mt<sup>++</sup> cells suggesting that mitochondrion-targeted CYP2E1 plays a role in alcohol-mediated mitochondrial dysfunction. In keeping with these results, both COS and Hep G2 cells expressing mitochondrion-targeted CYP2E1 showed significant loss of CcO activity, which was further reduced following alcohol treatment. These results further confirm and extend our previous studies that mitochondrion-targeted CYP2E1 augments alcohol-induced toxicity and mitochondrial dysfunction. One important observation in this study was the identification of CcO as a key mitochondrial target, which is probably the major cause of mitochondrial dysfunction.

Protein carbonylation is an important biomarker for oxidative stress-induced protein damage in various degenerative diseases. Carbonyl formation can occur by direct oxidation of amino acid side chains by ROS or they can be introduced indirectly through protein glycation and lipid peroxidation. We therefore assessed the relative levels of protein carbonylation by derivatization with DNP. Interestingly, both in alcohol-treated rat liver and Mt<sup>++</sup> cells treated with alcohol, we observed higher levels of protein carbonylation of the CcO complex. Notably, none of the other four complexes were carbonylated to any detectable level in Mt<sup>++</sup> cells even after alcohol treatment (Fig. 6B). These results provide direct and compelling evidence in support of our observation that CcO is a preferential target of CYP2E1-mediated alcohol toxicity.

It is increasingly realized that a major part of alcohol liver toxicity is elicited through oxidative stress. Metabolism of alcohol is known to involve formation of ROS, reactive nitrogen species, acetaldehyde, and other reactive metabolites (67–70). In addition, it is suggested that CYP2E1, which is one of the two major enzymes involved in alcohol metabolism, by itself generates ROS by inadvertent spillage of electrons because of its more open folded pattern (71, 72). Our results on complete or near complete reversal of CcO activity and oxidative stress conditions by mitochondrion-targeted antioxidants, Mito-Q and Mito-CP, indeed confirm that mitochondrially generated ROS (including NO) is a critical factor in alcohol-mediated mitochondrial dysfunction. Interestingly, DAS, a specific inhibitor of CYP2E1, also effectively reversed the loss of CcO activity in Mt<sup>++</sup> cells demonstrating that metabolic activity of CYP2E1 is essential for eliciting alcohol toxicity in the cell system.

Loss of CcO activity and attendant effects on mitochondrial function have been observed in a large number of diseases, including neurodegenerative diseases such as Alzheimer, myocardial ischemia, liver ischemia, cardiomyopathy, renal diseases, and cancer (29, 73–79). Doxorubicin, an anticancer drug,

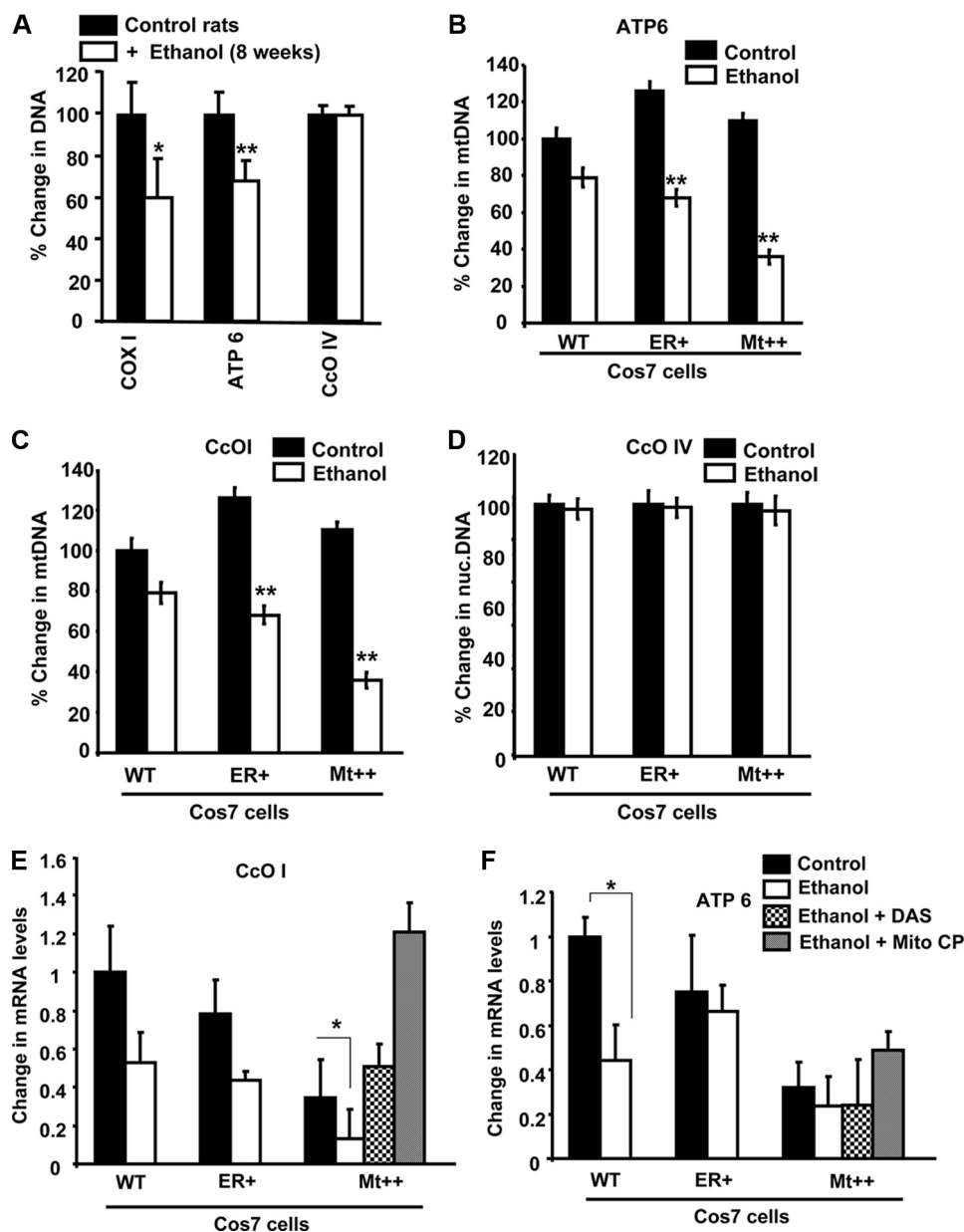


FIGURE 7. **Effects of alcohol treatment on mitochondrial DNA and mitochondrial mRNAs.** The mtDNA levels were determined using real time PCR using *Gapdh* DNA as the reference. *A*, mitochondrial DNA copy number in control pair-fed and alcohol-fed rat livers. *B* and *C*, effects of alcohol on mtDNA contents in cells expressing WT, ER<sup>+</sup>, and Mt<sup>++</sup> CYP2E1. *D*, effects of alcohol treatment on the levels of nuclear encoded *CcO1* gene. *E* and *F*, effects of alcohol on *CcO1* and *Atpase6* mRNA levels, respectively, in different cell lines. The effects of DAS (10  $\mu$ M) and mitochondrial antioxidant Mito-CP (2  $\mu$ M) on Mt<sup>++</sup> cells are indicated. Data represent mean  $\pm$  S.E. from three independent experiments. \* indicates  $p < 0.05$ , and \*\* indicates  $p < 0.001$ .

is known to induce cardiomyopathy as a secondary effect, which in turn is associated with mitochondrial dysfunction. It was shown that doxorubicin-induced cardiomyopathy involves direct association of the drug with heme a/a<sub>3</sub>, affecting CcO activity (80). In hypoxia and myocardial ischemia conditions, mitochondrial dysfunction was shown to be associated with loss of CcO activity (28, 31, 81), which was associated with selective loss of mitochondrion-encoded subunit I that houses the heme a/a<sub>3</sub> and copper centers, and nuclear gene-coded subunits IV1 and Vb (82–84). Protein phosphorylation was implicated in these losses (28, 31, 85–87). Interestingly, our results show the loss of the same two nucleus-encoded subunits (IV1 and Vb) in alcohol-treated Mt<sup>++</sup> cells and also in livers of rats fed with alcohol for <6 weeks (Fig. 5, *B* and *C*). It is likely that

protein phosphorylation or oxidative modification of subunits by mitochondrially generated ROS is the cause of subunit degradation. Results presented here show that the CcO complex is subject to a higher level of oxidative damage in response to alcohol treatment. The molecular mechanism of degradation of CcO subunits is currently under investigation.

It is now widely accepted that mitochondrial electron transport complexes, which couple respiration to ATP production, are organized in supramolecular complexes called respirosomes (45). This organization is thought to facilitate efficient transfer of electrons extracted from substrates, thus increasing the efficiency of transfer between complexes. The respirosome assembly is also thought to reduce leakage of electrons that can form reactive free radicals. Different combinations of complex

## Alcohol-induced Cytochrome Oxidase Dysfunction

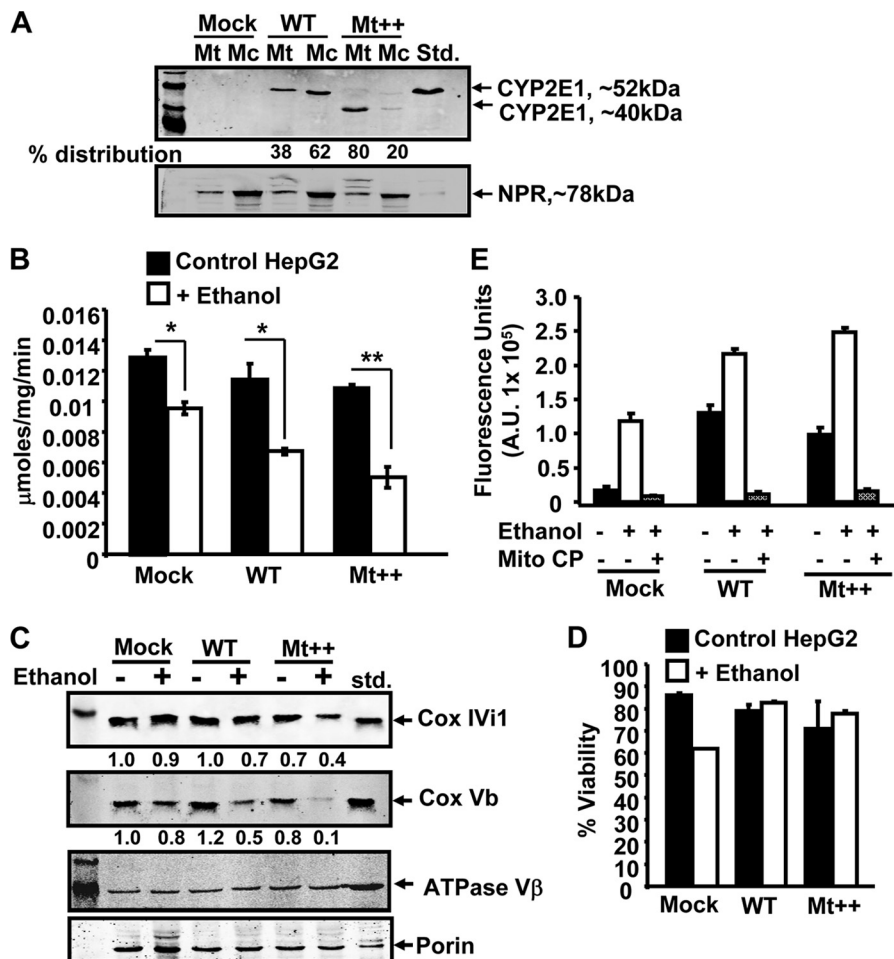


**FIGURE 8. Alcohol-mediated ROS production and loss of CcO activity in Hep G2 cells stably expressing WT and Mt<sup>++</sup> CYP2E1.** Hep G2 cells stably expressing CYP2E1 cDNAs were prepared as described under "Experimental Procedures." *A*, mitochondrial and microsomal fractions (50 μg of protein each) were subjected to immunoblot analysis using antibody to CYP2E1 protein. The blot was also co-developed with antibody to NADPH cytochrome P450 reductase (NPR) to assess relative cross-contamination. *B*, CcO activity was assayed with mitochondria from control and alcohol-treated cells (300 mM alcohol for 96 h). Results are mean ± S.E. of three independent experiments. *C*, mitochondrial proteins (50 μg each) from control and alcohol-treated cells were analyzed for CcO subunit IVi1 and Vb levels by immunoblot analysis using subunit-specific antibodies. The blot was also co-developed with porin antibody and antibody to ATPaseβ subunit used as a loading controls. The relative band intensities for CcO subunit IVi1 and Vb presented below respective blots represent average of two representative runs. *D*, % cell viability was determined for each cell type following ethanol treatment (300 mM for 96 h) as described under "Experimental Procedures." *E*, extracellular H<sub>2</sub>O<sub>2</sub> levels were measured using Amplex Red method as described under "Experimental Procedures." Ethanol treatment (300 mM) was for 96 h. Mito-CP (2 μM) was added 12 h before the measurement. Data represent mean ± S.E. of three independent measurements. \* indicates  $p < 0.05$  and \*\* indicates  $p < 0.001$ .

I, III, and IV are known to exist as super- and subcomplexes. Super complexes containing 1–4 copies of CcO have been described in bovine mitochondria. In this study, we show that cells expressing mitochondrion-targeted CYP2E1 (Mt<sup>++</sup> cells) contained markedly lower levels of super complexes than WT cells. Alcohol treatment caused a further depletion of super complexes. Treatment of rats with alcohol for <6 weeks had a similar effect on the hepatic mitochondrial content of respirosome complexes. Interestingly, in case of rat liver mitochondria, in addition to a general decrease in these complexes, there appears to be a differential effect on individual super complexes with S1 and S2, the two largest complexes more susceptible to alcohol-mediated damage. The alcohol-mediated damage to super complexes observed here may result in OXPHOS dysfunction, in addition to increased ROS formation.

In line with previous results, our results with CYP2E1-expressing cells also show loss of mtDNA and markedly reduced mitochondrial genome-encoded mRNA levels in alcohol-

treated cells. The alcohol effect is more severe in Mt<sup>++</sup> cells compared with ER<sup>+</sup> cells indicating that the extent of mtDNA loss is directly proportional to mitochondrial ROS production and oxidative stress. These DNA-damaging effects are reversibly less effective by DAS and a lot more effective by mitochondrion-targeted anti-oxidants, Mito-CP and Mito-Q (49, 50). We also see a similar loss of mtDNA and transcript levels in mitochondria from livers of alcohol-fed rats. We postulate that CcO is the immediate early target of CYP2E1 and alcohol-mediated toxicity. Loss of CcO activity further aggravates the oxidative stress conditions by increased ROS production by electron transport complexes either because of reverse electron flow or electron spillage as observed in CcO subunit Vb-depleted cells (28). The oxidative damage to mtDNA and other mitochondrial functional centers is possibly secondary to the CcO dysfunction.

Another noteworthy point is that despite a 30% reduction in mtDNA and mRNA contents in alcohol-fed rat livers, the levels

of complex I and complex III, as well their activities are affected only marginally. The CcO content and activity, however, is markedly reduced under these conditions. In the case of Mt<sup>++</sup> cells, a marked reduction of mtDNA and mitochondrially encoded mRNA levels are observed after alcohol treatment. Nevertheless, the complex I and complex III activities are not proportionately reduced. Increased stabilities of these complexes or altered turnover rates may be responsible for this effect. The CcO activity and complex levels, however, are selectively reduced by more than 70% suggesting more selective effects on this complex. We propose that an extreme sensitivity of CcO to mitochondrial ROS may be responsible for this selective effect.

In summary, our results on respirosome structures in alcohol-treated cells and livers imply a marked deficiency in mitochondrial OXPHOS, much more severe than previously envisioned. Our results also show that mitochondrial CYP2E1 plays a critical role in eliciting alcohol-mediated mitochondrial dysfunction, possibly by altering the CcO function. Damage to mitochondrial DNA and transcription may be secondary effects. Nearly complete recovery of these mitochondrial electron transfer complex and DNA damage by mitochondrion-targeted antioxidants and CYP2E1 inhibitors suggest possible ways to treat alcohol toxicity and tissue damage.

*Acknowledgments*—We acknowledge helpful comments and suggestions from laboratory members and Dr. Jan Hoek for providing alcohol-treated rats.

## REFERENCES

- Fromenty, B., Robin, M. A., Igoudjil, A., Mansouri, A., and Pessayre, D. (2004) The ins and outs of mitochondrial dysfunction in NASH. *Diabetes Metab.* **30**, 121–138
- Bailey, S. M. (2003) A review of the role of reactive oxygen and nitrogen species in alcohol-induced mitochondrial dysfunction. *Free Radic. Res.* **37**, 585–596
- Cunningham, C. C., Coleman, W. B., and Spach, P. I. (1990) The effects of chronic ethanol consumption on hepatic mitochondrial energy metabolism. *Alcohol Alcohol.* **25**, 127–136
- Hoek, J. B. (1994) Mitochondrial energy metabolism in chronic alcoholism. *Curr. Top. Bioenerg.* **17**, 197–241
- Coleman, W. B., and Cunningham, C. C. (1990) Effects of chronic ethanol consumption on the synthesis of polypeptides encoded by the hepatic mitochondrial genome. *Biochim. Biophys. Acta* **1019**, 142–150
- Cahill, A., Stabley, G. J., Wang, X., and Hoek, J. B. (1999) Chronic ethanol consumption causes alterations in the structural integrity of mitochondrial DNA in aged rats. *Hepatology* **30**, 881–888
- Cahill, A., Wang, X., and Hoek, J. B. (1997) Increased oxidative damage to mitochondrial DNA following chronic ethanol consumption. *Biochem. Biophys. Res. Commun.* **235**, 286–290
- Mantena, S. K., King, A. L., Andringa, K. K., Eccleston, H. B., and Bailey, S. M. (2008) Mitochondrial dysfunction and oxidative stress in the pathogenesis of alcohol- and obesity-induced fatty liver diseases. *Free Radic. Biol. Med.* **44**, 1259–1272
- Venkatraman, A., Landar, A., Davis, A. J., Chamlee, L., Sanderson, T., Kim, H., Page, G., Pompilius, M., Ballinger, S., Darley-Usmar, V., and Bailey, S. M. (2004) Modification of the mitochondrial proteome in response to the stress of ethanol-dependent hepatotoxicity. *J. Biol. Chem.* **279**, 22092–22101
- Harman, D. (1972) The biologic clock. The mitochondria? *J. Am. Geriatr. Soc.* **20**, 145–147
- Harman, D. (1973) Free radical theory of aging. *Triangle* **12**, 153–158
- Yakes, F. M., and Van Houten, B. (1997) Mitochondrial DNA damage is more extensive and persists longer than nuclear DNA damage in human cells following oxidative stress. *Proc. Natl. Acad. Sci. U.S.A.* **94**, 514–519
- Miquel, J., Economos, A. C., Fleming, J., and Johnson, J. E. (1980) Mitochondrial role in cell aging. *Exp. Gerontol.* **15**, 575–591
- Sanz, A., Pamplona, R., and Barja, G. (2006) Is the mitochondrial free radical theory of aging intact? *Antioxid. Redox. Signal.* **8**, 582–599
- Krähenbühl, S., Stucki, J., and Reichen, J. (1989) Mitochondrial function in carbon tetrachloride-induced cirrhosis in the rat. Qualitative and quantitative defects. *Biochem. Pharmacol.* **38**, 1583–1588
- Nozu, F., Takeyama, N., and Tanaka, T. (1992) Changes of hepatic fatty acid metabolism produced by chronic thioacetamide administration in rats. *Hepatology* **15**, 1099–1106
- Cederbaum, A. I., Lieber, C. S., and Rubin, E. (1974) Effects of chronic ethanol treatment of mitochondrial functions, damage to coupling site I. *Arch. Biochem. Biophys.* **165**, 560–569
- Bottenus, R. E., Spach, P. I., Filus, S., and Cunningham, C. C. (1982) Effect of chronic ethanol consumption of energy-linked processes associated with oxidative phosphorylation. Proton translocation and ATP-P<sub>i</sub> exchange. *Biochem. Biophys. Res. Commun.* **105**, 1368–1373
- Yang, S., Tan, T. M., Wee, A., and Leow, C. K. (2004) Mitochondrial respiratory function and antioxidant capacity in normal and cirrhotic livers following partial hepatectomy. *Cell. Mol. Life Sci.* **61**, 220–229
- Arai, M., Gordon, E. R., and Lieber, C. S. (1984) Decreased cytochrome oxidase activity in hepatic mitochondria after chronic ethanol consumption and the possible role of decreased cytochrome *aa*<sub>3</sub> content and changes in phospholipids. *Biochim. Biophys. Acta* **797**, 320–327
- Fiamingo, F. G., Jung, D. W., and Alben, J. O. (1990) Structural perturbation of the a<sub>3</sub>-CuB site in mitochondrial cytochrome *c* oxidase by alcohol solvents. *Biochemistry* **29**, 4627–4633
- Shiva, S., and Darley-Usmar, V. M. (2003) Control of the nitric oxide-cytochrome *c* oxidase signaling pathway under pathological and physiological conditions. *IUBMB Life* **55**, 585–590
- Venkatraman, A., Shiva, S., Davis, A. J., Bailey, S. M., Brookes, P. S., and Darley-Usmar V. M. (2003) Chronic alcohol consumption increases the sensitivity of rat liver mitochondrial respiration to inhibition by nitric oxide. *Hepatology* **38**, 141–147
- Kennedy, J. M. (1998) Mitochondrial gene expression is impaired by ethanol exposure in cultured chick cardiac myocytes. *Cardiovasc. Res.* **37**, 141–150
- Cifelli, P. M., Hargreaves, I., and Grünewald, S. (2002) Cytochrome oxidase deficiency in Lowe syndrome. *J. Inher. Metab. Dis.* **25**, 411–412
- Robinson, B. H. (2000) Human cytochrome oxidase deficiency. *Pediatr. Res.* **48**, 581–585
- DiMauro, S., Zeviani, M., Servidei, S., Bonilla, E., Miranda, A. F., Prella, A., and Schon, E. A. (1986) Cytochrome oxidase deficiency. Clinical and biochemical heterogeneity. *Ann. N.Y. Acad. Sci.* **488**, 19–32
- Galati, D., Srinivasan, S., Raza, H., Prabu, S. K., Hardy, M., Chandran, K., Lopez, M., Kalyanaraman, B., and Avadhani, N. G. (2009) Role of nuclearly encoded subunit Vb in the assembly and stability of cytochrome *c* oxidase complex: implications in mitochondrial dysfunction and ROS production. *Biochem. J.* **420**, 439–449
- Krieg, R. C., Knuedel, R., Schifmann, E., Liotta, L. A., Petricoin, E. F., 3rd, and Herrmann, P. C. (2004) Mitochondrial proteome. Cancer-altered metabolism associated with cytochrome *c* oxidase subunit level variation. *Proteomics* **4**, 2789–2795
- Kadenbach, B., Ramzan, R., and Vogt, S. (2009) Degenerative diseases, oxidative stress, and cytochrome *c* oxidase function. *Trends Mol. Med.* **15**, 139–147
- Prabu, S. K., Anandatheerthavarada, H. K., Raza, H., Srinivasan, S., Spear, J. F., and Avadhani, N. G. (2006) Protein kinase A-mediated phosphorylation modulates cytochrome *c* oxidase function and augments hypoxia and myocardial ischemia-related injury. *J. Biol. Chem.* **281**, 2061–2070
- Niranjan, B. G., Wilson, N. M., Jefcoate, C. R., and Avadhani, N. G. (1984) Hepatic mitochondrial cytochrome P-450 system. Distinctive features of cytochrome P-450 involved in the activation of aflatoxin B1 and benzo(a)pyrene. *J. Biol. Chem.* **259**, 12495–12501
- Yu, Q., Nguyen, T., Ogbi, M., Caldwell, R. W., and Johnson, J. A. (2008)

## Alcohol-induced Cytochrome Oxidase Dysfunction

- Differential loss of cytochrome *c* oxidase subunits in ischemia-reperfusion injury. Exacerbation of COI subunit loss by PKC- $\epsilon$  inhibition. *Am. J. Physiol. Heart Circ. Physiol.* **294**, H2637–H2645
34. Zaher, H., Buters, J. T., Ward, J. M., Bruno, M. K., Lucas, A. M., Stern, S. T., Cohen, S. D., and Gonzalez, F. J. (1998) Protection against acetaminophen toxicity in CYP1A2 and CYP2E1 double-null mice. *Toxicol. Appl. Pharmacol.* **152**, 193–199
  35. Guengerich, F. P., Kim, D. H., and Iwasaki, M. (1991) Role of human cytochrome P-450 IIE1 in the oxidation of many low molecular weight cancer suspects. *Chem. Res. Toxicol.* **4**, 168–179
  36. Bondoc, F. Y., Bao, Z., Hu, W. Y., Gonzalez, F. J., Wang, Y., Yang, C. S., and Hong, J. Y. (1999) Acetone catabolism by cytochrome P4502E1. Studies with CYP2E1-null mice. *Biochem. Pharmacol.* **58**, 461–463
  37. Ronis, M. J., Lindros, K. O., and Ingelman-Sundberg, M. (1996) in *Cytochromes P450, Pharmacological and Toxicological Aspects* (Ioannides, C., ed) pp. 211–239, CRC Press, Inc., Boca Raton, FL
  38. Sohn, O. S., Fiala, E. S., Requeijo, S. P., Weisburger, J. H., and Gonzalez, F. J. (2001) Differential effects of CYP2E1 status on the metabolic activation of the colon carcinogens azoxymethane and methylazoxymethanol. *Cancer Res.* **61**, 8435–8440
  39. Sumner, S. C., Fennell, T. R., Moore, T. A., Chanas, B., Gonzalez, F., and Ghanayem, B. I. (1999) Role of cytochrome P4502E1 in the metabolism of acrylamide and acrylonitrile in mice. *Chem. Res. Toxicol.* **12**, 1110–1116
  40. Bansal, S., Liu, C. P., Sepuri, N. B., Anandatheerthavarada, H. K., Selvaraj, V., Hoek, J., Milne, G. L., Guengerich, F. P., and Avadhani, N. G. (2010) Mitochondrion-targeted cytochrome P4502E1 induces oxidative damage and augments alcohol-mediated oxidative stress. *J. Biol. Chem.* **285**, 24609–24619
  41. Lieber, C. S., and De Carli, L. M. (1973) Ethanol dependence and tolerance. A nutritionally controlled experimental model in the rat. *Res. Commun. Chem. Pathol. Pharmacol.* **6**, 983–991
  42. Lowry, O. H., Rosebrough, N. J., Farr, A. L., and Randall, R. J. (1951) Protein measurement with the Folin phenol reagent. *J. Biol. Chem.* **193**, 265–275
  43. Wu, M., Neilson, A., Swift, A. L., Moran, R., Tamagnine, J., Parslow, D., Armistead, S., Lemire, K., Orrell, J., Teich, J., Chomicz, S., and Ferrick, D. A. (2007) Multiparameter metabolic analysis reveals a close link between attenuated mitochondrial bioenergetic function and enhanced glycolysis dependency in human tumor cells. *Am. J. Physiol. Cell Physiol.* **292**, C125–C136
  44. Birch-Machin, M. A., and Turnbull, D. M. (2001) Assaying mitochondrial respiratory complex activity in mitochondria isolated from human cells and tissues. *Methods Cell Biol.* **65**, 97–117
  45. Schagger, H., von Jagow, G. (1991) Blue native electrophoresis for isolation of membrane protein complexes in enzymatically active form. *Anal. Biochem.* **199**, 223–231
  46. Nijtmans, L. G., Taanman, J. W., Muijsers, A. O., Speijer, D., and Van den Bogert, C. (1998) Assembly of cytochrome *c* oxidase in cultured human cells. *Eur. J. Biochem.* **254**, 389–394
  47. Conard, C. C., Choi, J., Malakowsky, C. A., Talent, J. M., Dai, R., Marshall, P., and Gracy, R. W. (2001) Identification of protein carbonyls after two-dimensional electrophoresis. *Proteomics* **22**, 2046–2057
  48. Yu, H. L., Chertkow, H. M., Bergman, H., and Schipper, H. M. (2003) Aberrant profiles of native and oxidized glycoproteins in Alzheimer plasma. *Proteomics* **3**, 2240–2248
  49. James, A. M., Cochemé, H. M., Smith, R. A., and Murphy, M. P. (2005) Interactions of mitochondrion-targeted and -untargeted ubiquinones with the mitochondrial respiratory chain and reactive oxygen species. Implications for the use of exogenous ubiquinones as therapies and experimental tools. *J. Biol. Chem.* **280**, 21295–21312
  50. Dhanasekaran, A., Kotamraju, S., Karunakaran, C., Kalivendi, S. V., Thomas, S., Joseph, J., and Kalyanaraman, B. (2005) Mitochondria superoxide dismutase mimetic inhibits peroxide-induced oxidative damage and apoptosis. Role of mitochondrial superoxide. *Free Radic. Biol. Med.* **39**, 567–583
  51. Morimoto, M., Reitz, R. C., Morin, R. J., Nguyen, K., Ingelman-Sundberg, M., and French, S. W. (1995) CYP-2E1 inhibitors partially ameliorate the changes in hepatic fatty acid composition induced in rats by chronic administration of ethanol and a high fat diet. *J. Nutr.* **125**, 2953–2964
  52. Zeng, T., Zhang, C. L., Zhu, Z. P., Yu, L. H., Zhao, X. L., and Xie, K. Q. (2008) Diallyl trisulfide (DATS) effectively attenuated oxidative stress-mediated liver injury and hepatic mitochondrial dysfunction in acute ethanol-exposed mice. *Toxicology* **252**, 86–91
  53. Kono, H., Bradford, B. U., Yin, M., Sulik, K. K., Koop, D. R., Peters, J. M., Gonzalez, F. J., McDonald, T., Dikalova, A., Kadiiska, M. B., Mason, R. P., and Thurman, R. G. (1999) CYP2E1 is not involved in early alcohol-induced liver injury. *Am. J. Physiol.* **277**, G1259–G1267
  54. Wu, D., Cederbaum, A. I. (2009) Oxidative stress and alcoholic liver disease. *Semin. Liver Dis.* **29**, 141–154
  55. Bondy, S. C., and Guo, S. X. (1994) Effect of ethanol treatment on indices of cumulative oxidative stress. *Eur. J. Pharmacol.* **270**, 349–355
  56. Abdelmegeed, M. A., Moon, K. H., Chen, C., Gonzalez, F. J., and Song, B. J. (2010) Role of cytochrome P4502E1 in protein nitration and ubiquitin-mediated degradation during acetaminophen toxicity. *Biochem. Pharmacol.* **79**, 57–66
  57. Gonzalez, F. J. (2005) Role of cytochromes P450 in chemical toxicity and oxidative stress. Studies with CYP2E1. *Mutat. Res.* **569**, 101–110
  58. Lieber, C. S. (2004) Alcoholic fatty liver. Its pathogenesis and mechanism of progression to inflammation and fibrosis. *Alcohol* **34**, 9–19
  59. Morgan, K., French, S. W., and Morgan, T. R. (2002) Production of a cytochrome P4502E1 transgenic mouse and initial evaluation of alcoholic liver damage. *Hepatology* **36**, 122–134
  60. Lu, Y., Zhuge, J., Wang, X., Bai, J., and Cederbaum, A. I. (2008) Cytochrome P4502E1 contributes to ethanol-induced fatty liver in mice. *Hepatology* **47**, 1483–1494
  61. Lu, Y., Wu, D., Wang, X., Ward, S. C., and Cederbaum, A. I. (2010) Chronic alcohol-induced liver injury and oxidant stress are decreased in cytochrome P4502E1 knockout mice and restored in humanized cytochrome P4502E1 knock-in mice. *Free Radic. Biol. Med.* **49**, 1406–1416
  62. Butura, A., Nilsson, K., Morgan, K., Morgan, T. R., French, S. W., Johansson, I., Schuppe-Koistinen, I., and Ingelman-Sundberg, M. (2009) The impact of CYP2E1 on the development of alcoholic liver disease as studied in a transgenic mouse model. *J. Hepatol.* **50**, 572–583
  63. Wang, Y., Millonig, G., Nair, J., Patsenker, E., Stickle, F., Mueller, S., Bartsch, H., and Seitz, H. K. (2009) Ethanol-induced cytochrome P4502E1 causes carcinogenic etheno-DNA lesions in alcoholic liver disease. *Hepatology* **50**, 453–461
  64. Korourian, S., Hakkak, R., Ronis, M. J., Shelnett, S. R., Waldron, J., and Ingelman-Sundberg, M. (1999) Diet and risk of ethanol-induced hepatotoxicity: carbohydrate-fat relationships in rats. *Toxicol. Sci.* **47**, 110–117
  65. Aubert, J., Begriche, K., Knockaert, L., Robin, M. A., and Fromenty, B. (2011) Increased expression of cytochrome P450 2E1 in nonalcoholic fatty liver disease: mechanisms and pathophysiological role. *Clin. Res. Hepatol. Gastroenterol.* **35**, 630–637
  66. Knockaert, L., Descatoire, V., Vadrot, N., Fromenty, B., and Robin, M. A. (2011) Mitochondrial CYP2E1 is sufficient to mediate oxidative stress and cytotoxicity induced by ethanol and acetaminophen. *Toxicol. In Vitro* **25**, 475–484
  67. Lieber, C. S. (2005) Metabolism of alcohol. *Clinics in Liver Disease* **9**, 1–35
  68. Guengerich, F. P. (2003) Cytochromes P450, drugs, and diseases. *Mol. Interv.* **3**, 194–204
  69. Koop, D. R., and Coon, M. J. (1986) Ethanol oxidation and toxicity. Role of alcohol P-450 oxygenase. *Alcohol Clin. Exp. Res.* **10**, 44S–49S
  70. Lands, W. E. (1998) A review of alcohol clearance in humans. *Alcohol* **15**, 147–160
  71. Koop, D. R. (1992) Oxidative and reductive metabolism by cytochrome P4502E1. *FASEB J.* **6**, 724–730
  72. Mari, M., and Cederbaum, A. I. (2000) CYP2E1 overexpression in Hep G2 cells induces glutathione synthesis by transcriptional activation of  $\gamma$ -glutamylcysteine synthetase. *J. Biol. Chem.* **275**, 15563–15571
  73. DiMauro, S., and Schon, E. A. (2008) Mitochondrial disorders in the nervous system. *Annu. Rev. Neurosci.* **31**, 91–123
  74. Kadenbach, B., Arnold, S., Lee, I., and Hüttemann, M. (2004) The possible role of cytochrome *c* oxidase in stress-induced apoptosis and degenerative diseases. *Biochim. Biophys. Acta* **1655**, 400–408
  75. Betts, J., Lightowers, R. N., and Turnbull, D. M. (2004) Neuropathological

- aspects of mitochondrial DNA disease. *Neurochem. Res.* **29**, 505–511
76. Shoubridge, E. A. (2001) Nuclear genetic defects of oxidative phosphorylation. *Hum. Mol. Genet.* **10**, 2277–2284
77. Reeve, A. K., Krishnan, K. J., and Turnbull, D. (2008) Mitochondrial DNA mutations in disease, aging, and neurodegeneration. *Ann. N.Y. Acad. Sci.* **1147**, 21–29
78. Tanji, K., and Bonilla, E. (2000) Neuropathologic aspects of cytochrome *c* oxidase deficiency. *Brain Pathol.* **10**, 422–430
79. Beal, M. F. (2005) Mitochondria take center stage in aging and neurodegeneration. *Ann. Neurol.* **58**, 495–505
80. Chandran, K., Aggarwal, D., Migrino, R. Q., Joseph, J., McAllister, D., Konorev, E. A., Antholine, W. E., Zielonka, J., Srinivasan, S., Avadhani, N. G., and Kalyanaraman, B. (2009) Doxorubicin inactivates myocardial cytochrome *c* oxidase in rats. Cardioprotection by Mito-Q. *Biophys. J.* **96**, 1388–1398
81. Sayen, M. R., Gustafsson, A. B., Sussman, M. A., Molkentin, J. D., and Gottlieb, R. A. (2003) Calcineurin transgenic mice have mitochondrial dysfunction and elevated superoxide production. *Am. J. Physiol. Cell Physiol.* **284**, C562–C570
82. Kuo, W. W., Chu, C. Y., Wu, C. H., Lin, J. A., Liu, J. Y., Ying, T. H., Lee, S. D., Hsieh, Y. H., Chu, C. H., Lin, D. Y., Hsu, H. H., and Huang, C. Y. (2005) The profile of cardiac cytochrome *c* oxidase (COX) expression in an accelerated cardiac-hypertrophy model. *J. Biomed. Sci.* **12**, 601–610
83. Corbucci, G. C., Lettieri, B., Luongo, C., Orrù, A., Musu, M., and Marchi, A. (2006) Mitochondrial genome involvement in ischemia/reperfusion-induced adaptive changes in human myocardial cells. *Minerva Anesthesiol.* **72**, 337–347
84. Sharov, V. G., Todor, A. V., Imai, M., and Sabbah, H. N. (2005) Inhibition of mitochondrial permeability transition pores by cyclosporine A improves cytochrome *c* oxidase function and increases rate of ATP synthesis in failing cardiomyocytes. *Heart Fail. Rev.* **10**, 305–310
85. Bender, E., and Kadenbach, B. (2000) The allosteric ATP-inhibition of cytochrome *c* oxidase activity is reversibly switched on by cAMP-dependent phosphorylation. *FEBS Lett.* **466**, 130–134
86. Steenaart, N. A., and Shore, G. C. (1997) Mitochondrial cytochrome *c* oxidase subunit IV is phosphorylated by an endogenous kinase. *FEBS Lett.* **415**, 294–298
87. Fang, J. K., Prabu, S. K., Sepuri, N. B., Raza, H., Anandatheerthavarada, H. K., Galati, D., Spear, J., and Avadhani, N. G. (2007) Site-specific phosphorylation of cytochrome *c* oxidase subunits I, IV1 and Vb, in rabbit hearts subjected to ischemia/reperfusion. *FEBS Lett.* **581**, 1302–1310